Korean J. Chem. Eng., 39(12), 3350-3360 (2022)
DOI: 10.1007/s11814-022-1219-8

pISSN: 0256-1115
eISSN: 1975-7220

Heavy metal removal from aqueous solution by granular hydrated Portland cement

Peng Cheng*,,***, Yongxiang Ren*,**,†, Lei Yang*,**, Rituan Li*,**, Xue Wang*,**, Bin Li****, and Honglin Yuan*,****

*Key Laboratory of Northwest Water Resource, Environment and Ecology, MOE, Xi'an University of Architecture and Technology, Xi'an 710055, P. R. China
**Shaanxi Key Laboratory of Environmental Engineering, Xi'an University of Architecture and Technology, Xi'an 710055, P. R. China
***School of Civil Engineering, Nanyang Institute of Technology, Nanyang 473004, Henan Province, P. R. China
****Xi'an Botanical Garden, Xi'an 710061, Shaanxi Province, P. R. China
(*Received 28 February 2022 • Revised 27 June 2022 • Accepted 29 June 2022*)

Abstract−Granular hydrated Portland cement (HPC) was prepared as adsorbent to remove heavy metals in aqueous solution. Batch experiment results confirmed that heavy metals were removed through a combination of adsorption and precipitation. Adsorption played a more important role in the initial stage of the removal process or at lower concentrations of the heavy metals. After adsorption equilibrium was obtained in two days, the removal process continued for about three days due to the precipitation. Besides precipitation, the maximum Langmuir adsorption capacity reached 132.27, 87.14, 123.43 and 112.05 mg/g for Pb, Cu, Zn, and Cd, respectively. When various heavy metals coexisted, the removal capacity followed the order of Cu>Pb>Cd>Zn. The adsorption on the surfaces of HPC was mainly governed by surface precipitation and Ca^{2+} exchange, as suggested by XRD, SEM-EDS and released Ca^{2+} results. Most of the adsorbed heavy metals on the HPC and the precipitation formed in the liquid phase were stable under neutral and alkaline conditions. Overall, HPC particles exhibited a large potential for heavy metal removal. When cement-related materials containing HPC are employed for heavy metal removal, the dissolution of the precipitate at low pH might facilitate the migration of the heavy metals.

Keywords: Hydrated Portland Cement, Heavy Metal Removal, Adsorption, Precipitation

INTRODUCTION

Heavy metal pollution is one of the most serious environmental issues today. With the rapid development of industrial activity, large amounts of heavy metals are released into the environment. Heavy metals such as lead (Pb), copper (Cu), zinc (Zn), and cadmium (Cd), are potential threats to the global ecosystem and human health because of their toxic, non-biodegradable, and persistent nature [1-3]. The removal of heavy metals in the wastewater is important to further decrease the long-term accumulation in the ecological systems.

In recent years, many technologies, including chemical precipitation [4], ion-exchange [5,6], membrane filtration [7,8], coagulation and flocculation [9], and adsorption [10], have been investigated to remove heavy metals from aqueous solution. Among all the treatment technologies, adsorption is considered to be a flexible and efficient method to remove heavy metals from aqueous solution [11]. A wide variety of adsorbents such as activated carbon [12], nanomaterials [13,14] and mesoporous silica [15] were studied to remove heavy metals due to their large surface area and abundant binding sites. However, their relatively high production and modification cost encourage researchers to develop economical adsorbents.

Cement is one of the most commonly used engineering materials because of its cost effectiveness, easy availability and high strength. Various constituents in the HPC, such as calcium silicate hydrates (C-S-H), portlandite and ettringite, are produced in the hydration process of cement. These constituents have high adsorption potential for heavy metal cations due to their crystalline structure and relatively large specific surface area [16-18]. Recently, several cement-related materials have been investigated to adsorb heavy metal ions, including modified vermiculite concrete [19], zeolite-Portland cement mixture [20] and autoclaved aerated concrete [21]. However, the removal performance of HPC as heavy metals adsorbent was rarely reported. Without concrete aggregates, additives and other components in the material, the HPC has higher adsorption potential for heavy metals. The use of HPC in heavy metal removal is helpful to further evaluate and understand the adsorption performance, removal mechanism.

Precipitation was found in the removal of heavy metals by using permeable reactive concrete [22,23] and cement kiln dust [24-26], although heavy metal complexation, cation exchange and surface precipitation have often been supposed to be the main removal mechanisms for the cement-related materials. HPC also might provide OH^- and promote hydroxide precipitation of heavy metals in aqueous systems, which has received scant attention in previous studies. Hence, the contribution of precipitation should be given more attention in the heavy metal removal by HPC.

†To whom correspondence should be addressed.
E-mail: ryx@xauat.edu.cn
Copyright by The Korean Institute of Chemical Engineers.

HPC is also a typical constituent in construction and demolition waste. In recent years, recycled construction and demolition materials have been increasingly employed in constructed wetlands [27] and permeable pavements [28,29] for the treatment of stormwater runoff and other wastewater. The cement-related material in these systems has played a key role in removing heavy metals [19, 21,22]. Considering the long-term service of these water treatment facilities, better understanding of the accumulation of heavy metals is important to assess the removal performance and leaching risk in such practical application systems [30,31].

In this study, batch experiments were conducted to investigate the heavy metal removal performance by granular HPC. A facile method was employed to distinguish the precipitation in liquid phase and adsorption on the HPC particle surfaces. The removal performance of HPC particles for Pb, Cu, Zn and Cd ions in aqueous solutions was tested under various experimental conditions, such as contact time, initial concentration and pH. X-ray diffraction, Fourier transform infrared spectroscopy and scanning electron microscopy were applied to explore the removal mechanisms. The desorption performance of the heavy metal loaded HPC and the stability of the precipitate were tested to evaluate the leaching risk after adsorption.

MATERIALS AND METHODS

1. Chemicals and Granular HPC Preparation

All chemicals were of analytical grade and used as received without further purification in this study. $Pb(NO_3)_2$, $Cu(NO_3)_2{\cdot}3H_2O$, $Zn(NO_3)_2{\cdot}6H_2O$, $Cd(NO_3)_2{\cdot}4H_2O$ and other reagents were obtained from Tianjin Kermel Chemical Regent Co., Ltd.

Portland cement (P.C32.5R) was purchased from Shaanxi Qinling Cement Co. Ltd, China, with its compositions analyzed via X-Ray fluorescence (Table 1). It was hydrated with a water-to-cement ratio of 0.45. After a seven day curing under ambient temperature, the hardened cement paste was crushed and sieved to a particle size range of 1-2 mm. HPC particles were washed with deionized water, dried at 60 °C for 24 h, and stored in airtight polyethylene bags for later experiments.

2. Batch Removal Experiments

In a typical batch experiment, the initial pH of the heavy metal solutions was adjusted to 5±0.1, except the studies investigating the pH effects. Then, 0.05 g HPC particles were added to 200 ml Cu, Zn, Pb and Cd ions solutions in conical flasks, respectively. The mixture was agitated at 160 rpm in a thermostatic shaker for 48 h at 25 °C. Afterwards, samples were collected with a syringe for heavy metal measurement. All the experiments were performed in duplicate and the mean values were reported. All the pH adjustments in the experiments were performed by using 0.1 mol/L HCl and NaOH.

The removal capacity q_t (mg/g) and the removal efficiency E (%) of heavy metals were calculated according to Eq. (1) and Eq. (2), respectively:

$$q_t = \frac{C_0 - C_t}{m} \times V \tag{1}$$

$$E = \frac{C_0 - C_t}{C_0} \times 100\% \tag{2}$$

where m is the mass of the HPC (g), C_0 is the initial concentration of the heavy metal solution (mg/L), V is the volume of the solution (L), C_t is the concentration of heavy metal solution (mg/L) at time t (h). Samples withdrawn from the solutions were filtered immediately by a 0.22 μm membrane and measured to obtain C_t.

The effects of contact time were examined as aforementioned procedures with 0.05 g HPC in 200 ml solutions containing Pb, Cu, Zn and Cd ions at initial concentration of 100 mg/L. Samples were drawn periodically within seven days to obtain the concentration of heavy metals. The equilibrium experiments were carried out using similar conditions with the initial heavy metal concentrations ranging from 20 to 1,000 mg/L at 25 °C. The concentrations of Ca^{2+} were also tested in the equilibrium experiments to explore the relationship between the removal capacity and Ca^{2+} released by HPC particles. As for the influence of pH, the initial pH of the solutions containing 100 mg/L heavy metals was adjusted to the desired values in the range of 3.0-8.0. The simultaneous removal efficiency of HPC in multi-metal solutions containing the four heavy metals was tested. The initial concentrations of each heavy metal were set at 5, 25, and 50 mg/L (i.e., total metal concentration of 20, 100, and 200 mg/L), respectively.

Because of some small flocs observed in several solutions, the contribution of precipitation in the removal process was considered during the study for the effects of contact time and heavy metal concentration. To distinguish the heavy metals dissolved in the liquid phase and the metals precipitated as the suspended solid in the suspension, samples were first collected under vigorous stirring without filtration. Then, those without filtration were acidified with nitric acid (1 mol/L) to dissolve the suspended precipitate and tested for heavy metal concentration to obtain C_s (mg/L), which denotes the total heavy metals in the suspension. The heavy metals retained on the surface of HPC solids by adsorption, q_a (mg/g), can be determined by the following equation:

$$q_a = \frac{C_0 - C_s}{m} \times V \tag{3}$$

The removal of heavy metals through precipitation, q_p (mg/g), can be calculated by Eq. (4).

$$q_p = q_t - q_a \tag{4}$$

3. Tests of the Stability of the Removed Heavy Metals

Desorption property was examined to determine the stability of

Table 1. Chemical composition of P.C32.5R cement (wt%)

CaO	SiO_2	Fe_2O_3	Al_2O_3	SO_3	MgO	K_2O	MnO	P_2O_5	TiO_2	ZnO	Others
67.15	17.02	5.08	3.52	3.17	1.81	0.76	0.47	0.30	0.29	0.11	0.32

heavy metals adsorbed on the HPC. Desorption experiments were performed by first adding 0.05 g HPC into 200 ml heavy metal solution at initial concentration of 100 mg/L, and shaking for five days. Then, the heavy metal saturated HPC particles were separated and rinsed with deionized water three times. Afterwards, they were added to HCl, NaOH and $CaCl_2$ solutions at the concentration of 0.1 mol/L and the dosage of 0.01 g/L, respectively. The mixtures were shaken at 160 rpm in a thermostatic shaker at 25 °C. After 2 h contact time, the samples were collected and measured for heavy metal concentration. The desorption percentage E_d (%) was calculated using the following equation:

$$E_d = \frac{C \times V}{m_d \times q_e} \times 100\% \quad (5)$$

where C is the heavy metal concentration of the desorption solution (mg/L), V is the volume of the solution (L), m_d is the mass of the heavy metals saturated HPC (g), q_e is adsorption capacity (mg/L) at equilibrium.

The stability of the precipitate was assessed by comparing the turbidity and the heavy metal concentration of the suspensions at different pH values. Heavy metals were removed under similar conditions before the desorption experiments. After the removal, the suspensions were collected and adjusted to pH values varying from 3.0 to 9.0. Then samples were collected to obtain the turbidity and heavy metal concentration.

4. Analytical Methods

Concentrations of Pb, Cu, Zn, Cd and Ca were determined by flame atomic absorption spectroscopy (Thermo Fisher iCE3000 spectrometer, USA). The specific surface area and porosity of HPC were analyzed by N_2 adsorption-desorption method at 77 K with a gas adsorption analyzer (TriStar 3000, Micromeritics, USA). The crystal structure of HPC before and after the removal process and the heavy metal precipitate was tested by X-ray diffraction (XRD) on a DMAX-2400X diffractometer (Rigaku Corporation, Japan) with Cu Ka radiation. XRD patterns were obtained from 5-90° at a scan speed of 4°/min. Fourier transform infrared spectroscopy (FTIR) (IRPrestige-21, Shimadzu Corporation, Japan) was applied to explore the functional groups with the scanning range from 400 to 4,000 cm^{-1}. The morphology of HPC was examined by scanning electron microscope (SEM) coupled with energy dispersive X-ray spectroscopy (EDS) (JSM-6510LV, JEOL Ltd., Japan).

RESULTS AND DISCUSSION

1. Characterization of HPC

The SEM image and EDS spectrum of the prepared HPC are shown in Fig. 1. The HPC particles presented rough, porous surfaces. The irregular granules might be related to the C-S-H phases, which were produced in the hydration of Portland cement. The EDS spectrum of HPC showed the presence of elements such as C, O, Ca, Si, Al, Fe, S, Mg and K, which was in accordance with the X-Ray fluorescence analysis of the purchased Portland cement. The N_2 adsorption-desorption isotherms presented type IV isotherms with H2 hysteresis loop (see Fig. S1), indicating the mesoporous structure of HPC [32,33]. The surface area of HPC particles was calculated to be 29.13 m^2/g, according to Brunauer-Emmett-Teller (BET) method.

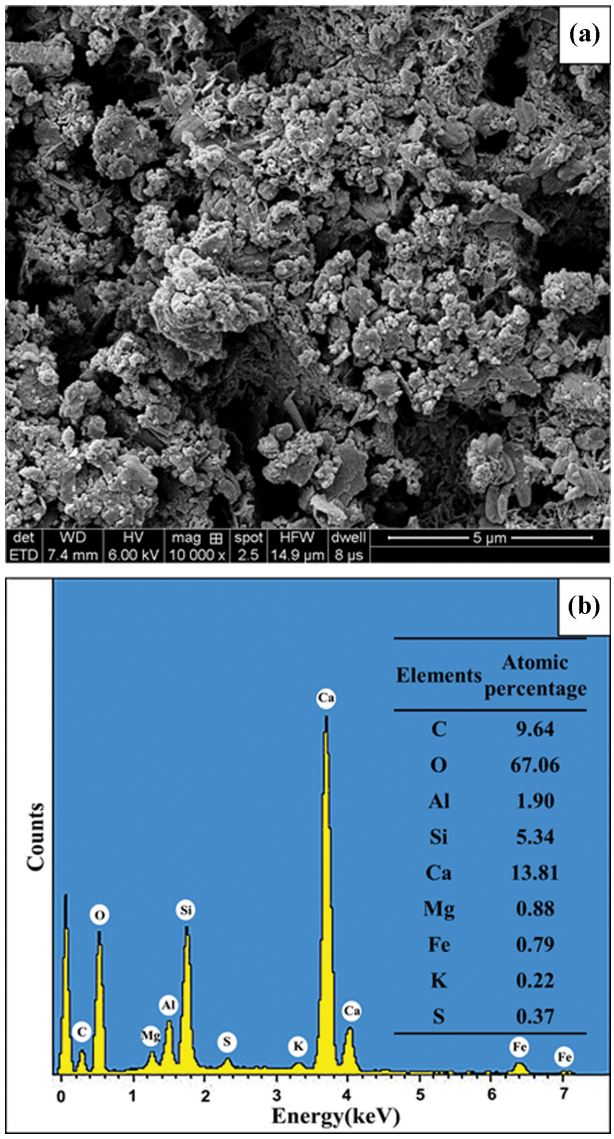


Fig. 1. SEM image (a) and EDS spectrum (b) of the prepared HPC.

2. Effect of Contact Time

The effect of contact time on the removal capacity of Pb, Cu, Zn and Cd is shown in Fig. 2. Both adsorption and precipitation were observed in the removal process. During the first 24 h, the removal of Pb, Cu, Zn and Cd was mainly contributed by adsorption, accounting for 54.79%, 77.93%, 80.43% and 85.93% of the total removal capacity, respectively. The adsorption reached equilibrium within about 48 h. As the reaction continued, the total removal capacity became obviously larger than the adsorption capacity. In particular, the total removal capacity for Pb ions reached 375 mg/g in five days, approximately four-fold of the adsorption capacity.

The proportion of adsorption and precipitation was also influenced by the contact time. The initial removal rate was fast due to the large number of vacant surface sites available for adsorption. With the adsorption equilibrium obtained, the precipitation process began to play a more important role. The removal of heavy met-

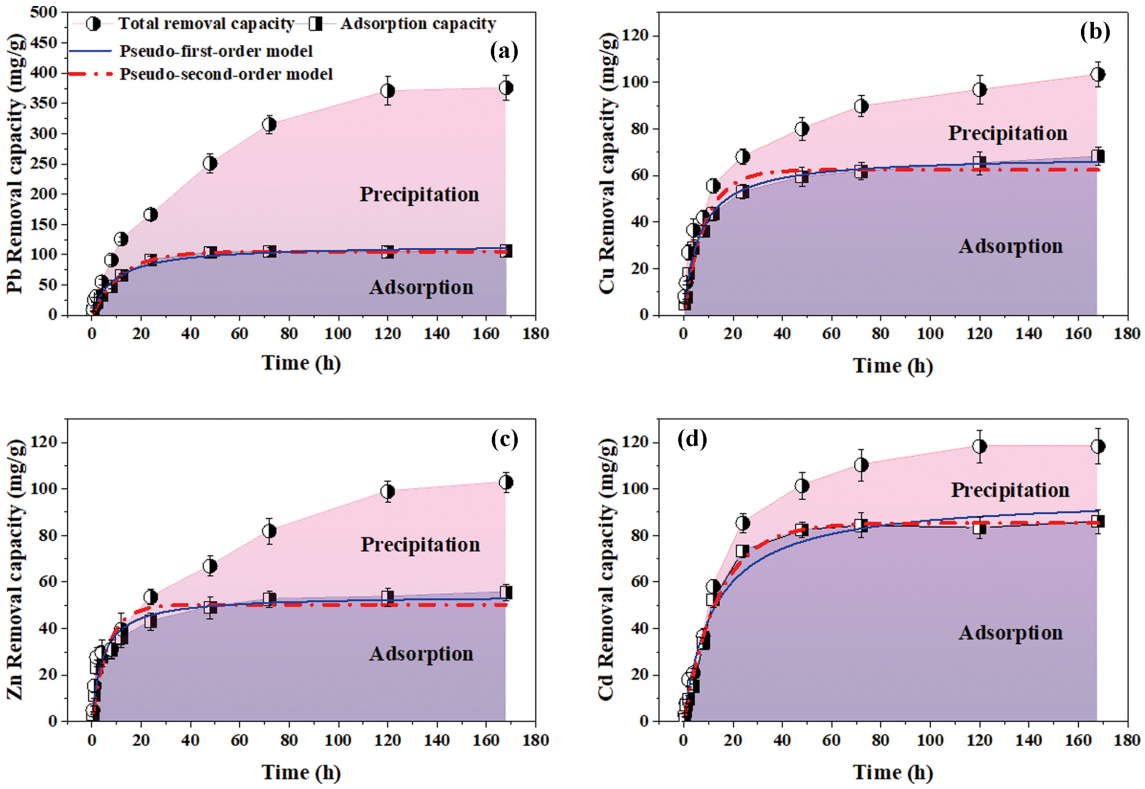


Fig. 2. Effect of contact time on the removal of heavy metals. (a) Pb; (b) Cu; (c) Zn; (d) Cd.

Table 2. Kinetic model fitting parameters

Heavy metals	Pseudo-first-order kinetics			Pseudo-second-order kinetics		
	Q_e (mg/g)	K_1 (1/h)	R^2	Q_e (mg/g)	K_2 (g/mg·h)	R^2
Pb	105.14	0.085	0.9890	116.50	0.001	0.9846
Cu	62.46	0.115	0.9682	68.52	0.002	0.9949
Zn	50.23	0.156	0.8974	54.21	0.004	0.9629
Cd	85.38	0.070	0.9925	97.05	0.001	0.9739

als continued for about five days through a combination of adsorption and precipitation.

To evaluate the adsorption performance, pseudo-first-order and pseudo-second-order models were employed to fit the adsorption results. They can be expressed in Eq. (6) and Eq. (7), respectively:

$$q_a = q_e(1-e^{-k_1 t}) \quad (6)$$

$$q_a = \frac{q_e^2 k_2 t}{1+k_2 q_e t} \quad (7)$$

where q_a (mg/g) is the adsorption amount at any given time t (h), q_e (mg/g) is the adsorption capacity at equilibrium, k_1 (1/h) and k_2 (g/mg·h) are the rate constants of the pseudo-first-order and pseudo-second-order models, respectively.

As depicted in Fig. 2, the adsorption kinetics data were fitted well with both the pseudo-first-order and pseudo-second-order models, indicating that the adsorption process on HPC might be controlled by chemical adsorption as well as mass transport [16, 34]. The kinetic model parameters are shown in Table 2. The fitting rate constants of Pb, Cu, Zn and Cd indicated different characteristics of the four heavy metals.

The adsorption capacity of HPC and other low-cost adsorbents for heavy metal removal, as well as the experiment conditions, is listed in Table 3. Even though the proportions of precipitation were not considered, the adsorption capacity of HPC particles was higher than other modified mineral materials, such as montmorillonite [35], alkaline Ca-bentonite [36], and iron-coated zeolite [37]. For the reported cement-related adsorbents, such as zeolite-Portland cement mixture [20], sulfate aluminate cement amended bentonite [38], modified vermiculite concrete [19] and autoclaved aerated concrete [21], HPC is comparable to most of them in terms of adsorption capacity.

Table 1 also shows that the particle diameter (1-2 mm) and specific surface areas (29.13 m^2/g) limited the adsorption kinetics of HPC. The relatively long equilibrium time (48 h) may restrict the application of HPC in a traditional adsorption column. In fact, most of the low-cost adsorbents in Table 3 have difficulty in regeneration and are not suitable for the adsorption column. Compared

Table 3. Comparison of the adsorption capacity of various reported low-cost adsorbents

Adsorbents	Heavy metals	Adsorption capacity (mg/g)	Initial concentration (mg/L)	Contact time (h)	Morphology
HPC	Pb	103.56	100	48	Particle (1-2 mm)
	Cu	59.42			
	Zn	49.06			
	Cd	82.35			
Montmorillonite [35]	Pb	31.10	50	3	Powder
	Cd	30.70		4	
Alkaline Ca-bentonite [36]	Zn	149	100	2.5	Powder
Iron-coated zeolite [37]	Pb	11.16	50	24	Powder
	Cu	9.33			
	Zn	6.22			
	Cd	7.24			
C-S-H based nanocomposites [16]	Pb	508	300	6	Powder
	Cu	244			
	Zn	273			
Sulphate aluminate cement amended bentonite [38]	Pb	123.14	180	2	Particle (0.15 mm)
	Cd	125.07			
Modified vermiculite concrete [19]	Pb	197.6	200	2	Particle (1.5-2.5 mm)
	Cd	36.0			
	Cu	53.2			
Zeolite-Portland cement mixture [20]	Pb	27.03	1,600	1	Particle (2 mm)
	Cu	23.25			
	Zn	12.85			
	Cd	10.87			
Autoclaved aerated concrete [21]	Pb	257.0	2,000	24	Particle (0.1-2 mm)
	Cd	16.5			(0.1-2 mm)

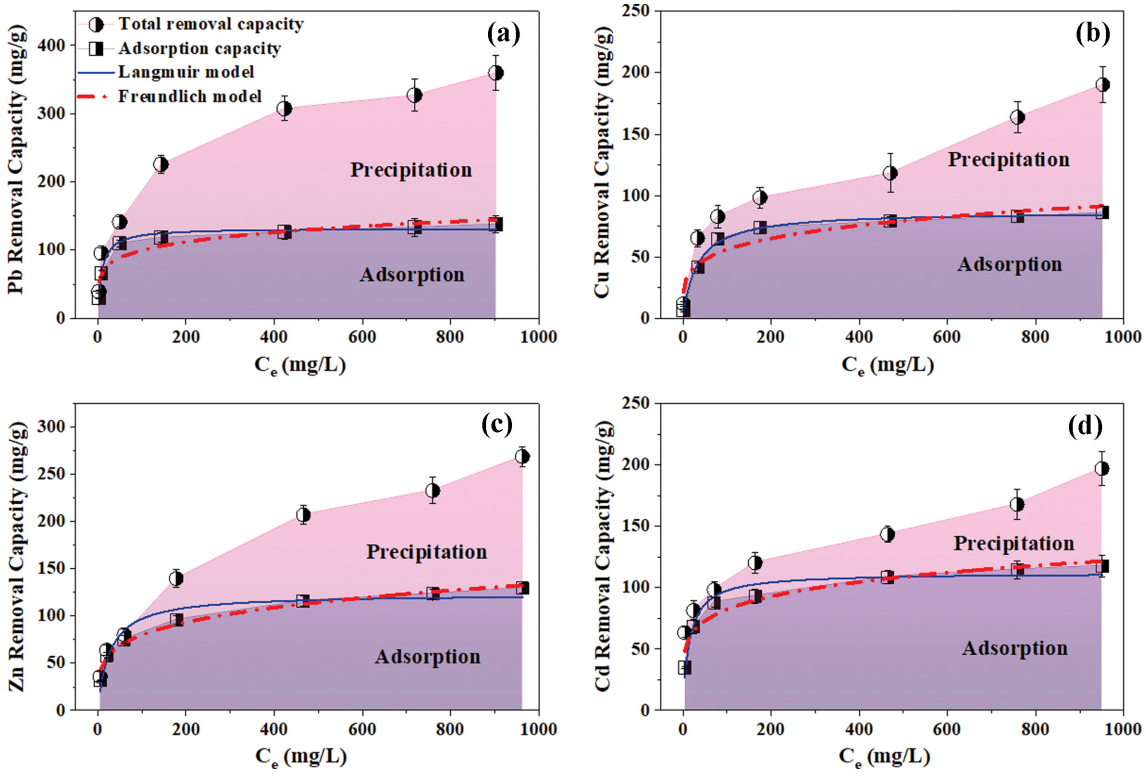


Fig. 3. Effect of equilibrium concentration on the removal of heavy metals. (a) Pb; (b) Cu; (c) Zn; (d) Cd.

with the powder materials in Table 3, the granular HPC exhibits higher hydraulic conductivity [39]. Hence, granular HPC is more suitable as low-cost material for applications such as constructed wetlands and permeable pavement systems, which will exhibit heavy metal removal performance for a long time.

3. Effect of Heavy Metal Concentration

As presented in Fig. 3, the total removal of heavy metals increased with the increase of equilibrium concentration. When the equilibrium concentration was lower than 100 mg/L, adsorption played a more important role than precipitation, which accounted for about more than 70% of the total removal capacity. The adsorption capacity reached plateaus at the equilibrium concentration of about 200 mg/L. However, the total removal capacity of HPC increased during the whole test, suggesting the enhanced precipitation processes at higher concentrations. After the adsorption sites were saturated, precipitation further enhanced the removal performance.

Adsorption isotherm models are extensively used to depict the relationship between adsorbent and adsorbate under equilibrium conditions [40]. Langmuir and Freundlich adsorption isotherm models were employed to simulate the adsorption data of Pb, Cu, Zn, and Cd ions on HPC in this study. The nonlinear forms of the Langmuir and Freundlich model are described in Eq. (8) and Eq. (9), respectively:

$$q_e = \frac{Q_m k_L C_e}{1 + k_L C_e} \tag{8}$$

$$q_e = k_F C_e^{1/n} \tag{9}$$

where q_e (mg/g) is the adsorption capacity at equilibrium, Q_m (mg/g) is the maximum adsorption capacity, k_L (L/mg) is the Langmuir adsorption constant, C_e (mg/g) is the heavy metal solution concentration at equilibrium, k_F ((mg/g)(L/mg)$^{1/n}$) and 1/n are the Freundlich adsorption constants.

The adsorption isotherm fitting results are shown in Fig. 3 and Table 4. In general, Langmuir adsorption isotherm models fitted the adsorption data well with the correlation coefficient (R^2) ranging from 0.927 to 0.993. Based on the Langmuir isotherm parameter, the maximum adsorption capacity was 132.27, 87.14, 123.43 and 112.05 mg/g for Pb, Cu, Zn, and Cd, respectively. That for Pb was the larger than other heavy metals, which was consistent with the kinetics experiment result. Compared with Langmuir isotherm model, the fitting correlation coefficients (R^2) of Freundlich adsorption isotherm model were lower in a range of 0.842-0.923. The values of 1/n in the Freundlich model for Pb, Cu, Zn, and Cd ions were less than 1, suggesting that adsorption occurred easily [38].

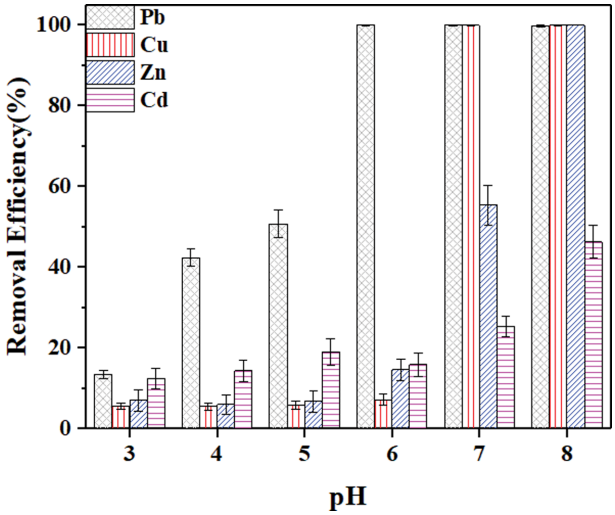


Fig. 4. Effect of pH on the removal efficiency of heavy metals.

4. Effect of Solution pH

The effect of the initial solution pH on the removal of heavy metals by HPC is shown in Fig. 4. In general, the removal efficiency of the heavy metals increased with the rise of pH value. Besides, Pb presented a higher removal efficiency than others and almost all the Pb was removed in the pH range of 6-8. These results are consistent with those by other studies [20,41].

The pH has a significant impact on the uptake of heavy metals, since it affects the surface charge of the HPC, the aqueous speciation of the heavy metals and the formation of precipitates [42]. Solution pH influences the hydrolysis of divalent metal ions (M^{2+}), resulting in the formation of different metal ions speciation, such as $M(OH)^+$, $M_2(OH)_2^{2+}$, $M_3(OH)_4^{2+}$, $M(OH)_2$ and $M(OH)_3^-$ [41]. The changes of heavy metal speciation distribution at different pH values might affect the ion radius and the adsorption affinity, which in turn affects the removal capacity. The observed smaller removal of heavy metals in low pH conditions might also be attributed to the competition of H^+ with metal ions for adsorption sites and the less formation of hydroxide precipitation [34]. At high pH condition, precipitates form easily because the heavy metal cations might react with carbonate ions dissolved from the air or hydroxide ions (OH^-) [21,43].

5. Multi-metal Solution Removal

The removal performance of HPC at initial heavy metal concentrations of 5 mg/L, 25 mg/L and 50 mg/L in multi-metal aqueous solutions was investigated. The results are shown in Fig. 5 and compared with the removal efficiency at 100 mg/L single-metal

Table 4. Langmuir and Freundlich isotherm fitting parameters

Heavy metals	Langmuir			Freundlich		
	Q_m (mg/g)	K_L (L/mg)	R^2	K_F ((mg/g)(L/mg)$^{1/n}$)	1/n	R^2
Pb	132.27	0.11	0.986	45.95	0.17	0.842
Cu	87.14	0.03	0.993	20.51	0.22	0.872
Zn	123.43	0.04	0.927	28.63	0.22	0.914
Cd	112.05	0.07	0.940	37.11	0.17	0.923

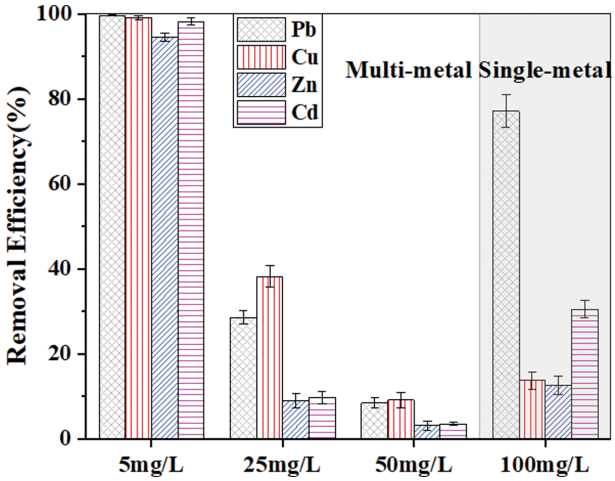


Fig. 5. Heavy metal removal efficiency by HPC in multi-metal and single-metal aqueous solutions at different initial concentration.

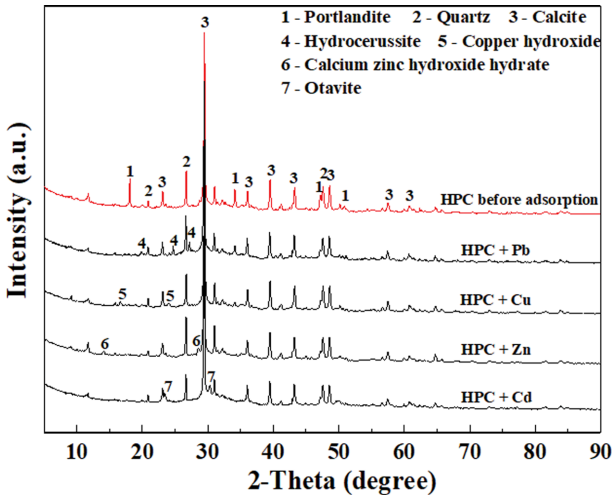


Fig. 6. XRD patterns of HPC before and after the heavy metal adsorption.

solutions. The removal efficiency presented Pb>Cd>Cu>Zn sequence at the concentration of 100 mg/L in the single metal solutions. In multi-metal aqueous solutions, the removal efficiency of Pb and Cu was higher than that of Zn and Cd.

These results were different with the removal efficiencies in the single metal solutions due to relatively less removed Cu. The discrepancy of the order between the single- and multi-metal systems might be due to different proportions of Cu speciation. Greater proportions of $Cu(OH)^+$, $Cu(OH)_3^-$, and $Cu(OH)_2$ (aq) were formed in the multi-element system than the single-element system in a previous study [44].

When various heavy metals coexist, the removal of Pb and Cu is better than that of Zn and Cd, which was also observed in the works using adsorbents such as zeolite [37], fly ash [42], and kaolinite [44]. A possible explanation is that the selectivity series are affected by the tendency of hydration and hydrolysis of heavy metals [44]. Pb and Cu ions interact faster with the adsorbent surface because their hydration is more readily [21]. Previous studies have shown that the characteristics of heavy metals, such as the first hydrolysis constant (pK_1), electronegativity, hydrated ion radius and other factors, have important effects on the sequence of removal selectivity [19,45]. The adsorption affinity decreases with the increase of pK_1 and the hydrated radius of the heavy metals. In the meantime, adsorption selectivity is greater with higher electronegativity [46,47]. In this study, the competitive removal of these four heavy metals was the result of the combined effect of heavy metals characteristics and HPC properties.

6. Removal Mechanism

To explore the adsorption mechanism, the HPC particles before and after the removal were characterized by XRD, FT-IR and SEM-EDS. The concentrations of the released Ca^{2+} in the solutions and the XRD patterns of the precipitate were also tested to investigate chemical precipitation occurred in the liquid phase.

The XRD patterns of HPC before and after the four heavy metals adsorption are shown in Fig. 6. The main mineral phases of calcite ($CaCO_3$, PDF 05-0586) and quartz (SiO_2, PDF 46-1045) were identified in all XRD patterns. However, the reflection intensity of Portlandite ($Ca(OH)_2$, PDF 44-1481) decreased after adsorption, indicating that the Portlandite might dissolve and release Ca^{2+} and OH^- into the solutions. Some inconspicuous peaks were found in the XRD patterns after treating heavy metals solutions, suggesting new phases such as hydrocerussite ($Pb_3(CO_3)_2(OH)_2$, PDF 13-0131), copper hydroxide ($Cu(OH)_2$, PDF 13-0420), calcium zinc hydroxide hydrate ($Ca(Zn(OH)_3)_2{\cdot}2H_2O$, PDF 24-0222) and otavite ($CdCO_3$, PDF 42-1342) might be formed by surface precipitation. Pb, Cu, Zn and Cd ions might precipitate in alkaline environments with Ca^{2+} and CO_3^{2-} in the aqueous solutions, which is consistent with previous studies [16,21,48].

The FTIR spectra depicted in Fig. S2 were in accordance with the XRD analyses. The similar FTIR spectra before and after adsorption confirmed that the structure of HPC was well retained in the removal of heavy metals. The bands visualized in the spectrum at 445-455 and 963-970 cm^{-1} correspond to the bending vibration and the asymmetric stretching vibration of Si-O bond, which are closely related to SiO_4 tetrahedra in HPC [16,49]. The bands at 711, 873-875 and 1,418-1,439 cm^{-1} were assigned to carbonate phases [48,50], which were also identified in XRD patterns.

The SEM images of HPC loaded with Pb, Cu, Zn and Cd are shown in Fig. 7. There are obvious changes between the surface of HPC samples before and after adsorption. The porosity of the HPC is clearly visible before treatment with heavy metals (Fig. 1(a)). After adsorption, the voids are filled and the morphology of HPC shows denser surfaces with different crystals or amorphous structures. Additionally, the original irregular surfaces became relatively uniform. Several structures with shapes such as flakes, granules and nets were formed, respectively, suggesting the possible surface precipitation identified by XRD analysis.

The atomic percentage of Pb, Cu, Zn, and Cd on the surface of HPC after adsorption was detected to be 10.52%, 19.36%, 21.06% and 13.20% in the energy spectrum analysis (Fig. S3), respectively. The results indicate the successful adsorption of these four heavy metal ions. Both C-S-H and Portlandite in HPC particles might

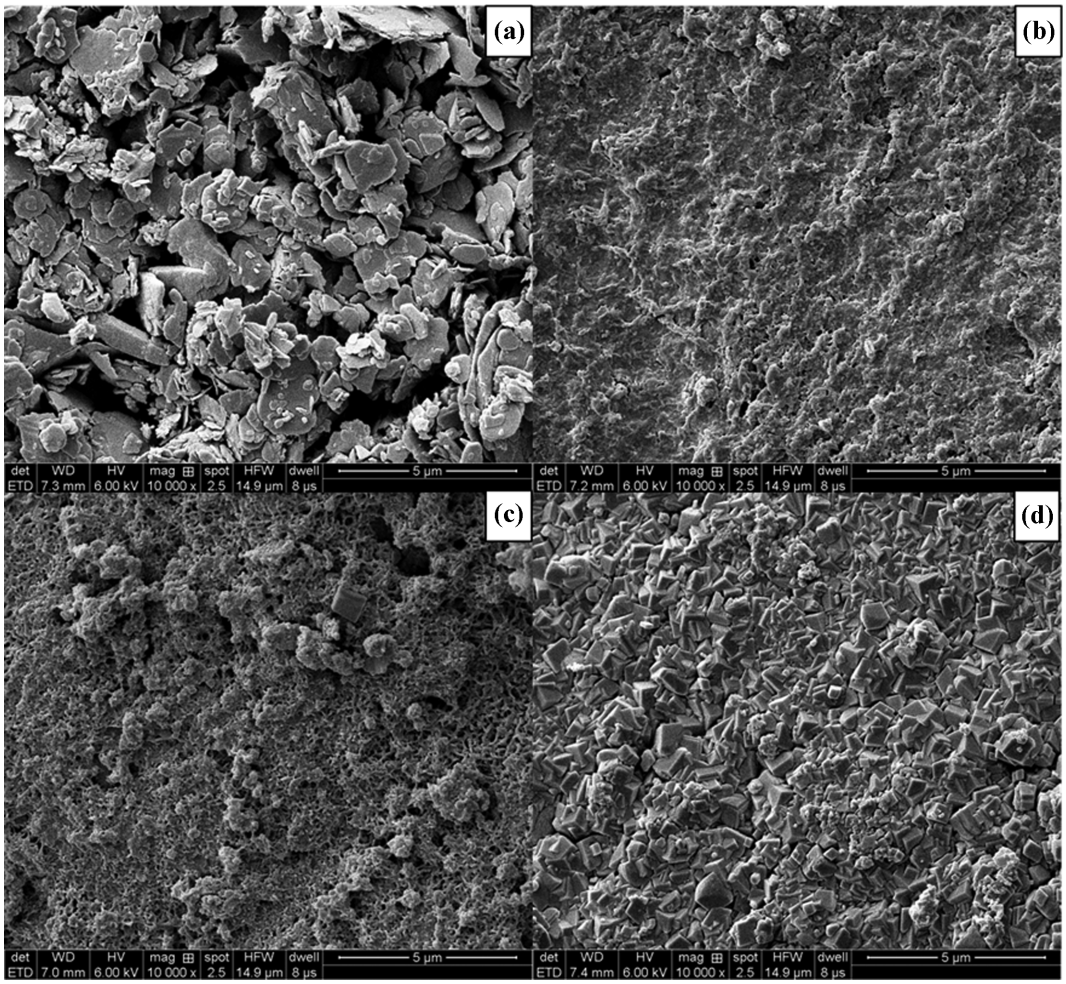


Fig. 7. SEM images of HPC loaded with Pb (a), Cu (b), Zn (c), Cd (d).

release Ca^{2+} into aqueous solution [16]. Compared with the HPC before adsorption (Fig. 1(b)), the atomic percentage of Ca decreased from 13.81% to the range of 0.41%-2.62% after the adsorption. This observed decrease of Ca and the presence of heavy metals in EDS analyses suggests the possible exchange of Ca^{2+} during the adsorption process.

The released Ca^{2+} was also tested for seven days in the batch experiments. The removal capacity of the four heavy metals shows positive linear relationships with the concentrations of the released Ca^{2+} (see Fig. S4). The fitting linear correlation coefficient (R^2) of Pb, Cu, Zn, and Cd is 0.937, 0.964, 0.867, and 0.946, respectively. In addition to the dissolution of Portlandite, the released Ca^{2+} might also come from the C-S-H phases in the HPC particles. The C-S-H has shown the potential to remove bivalent cations through exchanging with Ca^{2+} in earlier studies [21,51]. Furthermore, because of the Ca^{2+} released from HPC particles to the heavy metal solutions, special attention should be paid to anti-corrosion measures in heavy metal wastewater treatment facilities by using concrete materials.

The XRD patterns of the precipitates were collected to elucidate the crystal structures and phase compositions. As presented in Fig. 8, in the precipitates of Pb and Cd, cerussite ($PbCO_3$, PDF 47-1734), hydrocerussite ($Pb_3(CO_3)_2(OH)_2$, PDF 13-0131), calcite ($CaCO_3$, PDF 47-1734) and otavite ($CdCO_3$, PDF 42-1342) are clearly identified. However, the intensity of Cu and Zn precipitates is much

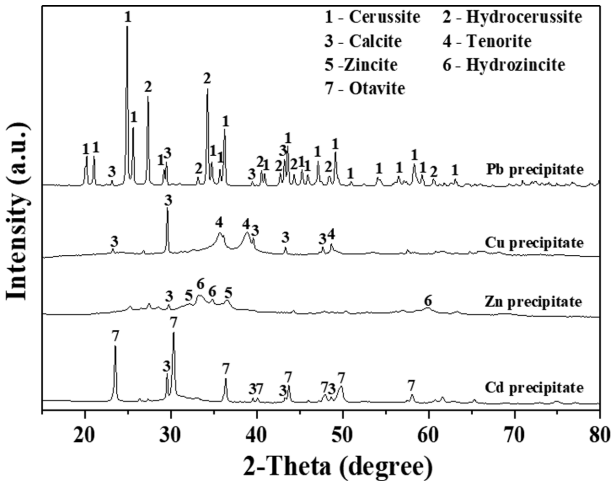


Fig. 8. XRD patterns of the precipitates formed in the removal process.

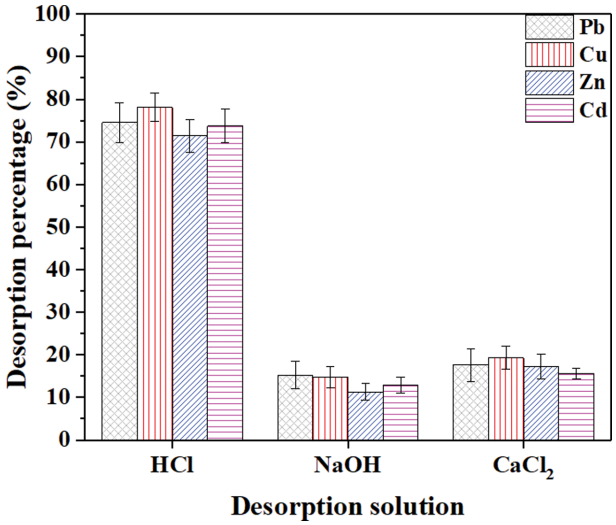


Fig. 9. Desorption percentages of the heavy metals loaded HPC with different solutions.

lower than that of Pb and Cd. Only some inconspicuous peaks of Tenorite (CuO, PDF 48-1548), Zincite (ZnO, PDF 75-1526) and Hydrozincite ($Zn_5(OH)_6(CO_3)_2$, PDF 72-1100) can be found in the Cu and Zn precipitates. The crystallinity of different heavy metal precipitation varies widely. The mineral composition of the precipitate is consistent with the results obtained in earlier research [43]. The OH^- and Ca^{2+} released from the HPC precipitated the heavy metals in batch removal process. Because the carbonates were confirmed by the XRD patterns, CO_2 from the ambient atmosphere may also be involved in the precipitation.

According to the above results and analysis, the removal of heavy metals by HPC particles mainly involves two processes. First, chemical precipitation occurred in the liquid phase. The heavy metal ions precipitated by the released OH^- and Ca^{2+} from C-S-H and portlandite. The contribution of precipitation to the total removal capacity is clearly shown in Fig. 2 and Fig. 3. Second, there was also adsorption of the heavy metal ions on the surfaces of HPC particles, which mainly dominated by of Ca^{2+} exchange and surface precipitation. This was suggested by XRD, SEM-EDS and released Ca^{2+} results.

7. Stability of the Removed Heavy Metals

The heavy metal removal performance of HPC suggests the potential utilization of the cement-related materials in constructed wetlands and permeable pavement systems. Considering the long-term service of these facilities and the precipitation formation, the stability of the removed heavy metals was tested to assess leaching risk in such systems.

As shown in Fig. 9, more than 70% of the adsorbed heavy metals in 0.1 mol/L HCl solutions were dissolved from the surface of the HPC. While the desorption percentage by $CaCl_2$ and NaOH solutions was lower than 20% for all four heavy metals. The desorption results are consistent with the effect of pH on the removal performance. Most of the adsorbed heavy metals on HPC were stable under neutral and alkaline conditions. However, the heavy metals loaded HPC might release heavy metal ions under acidic conditions and increase environmental risks.

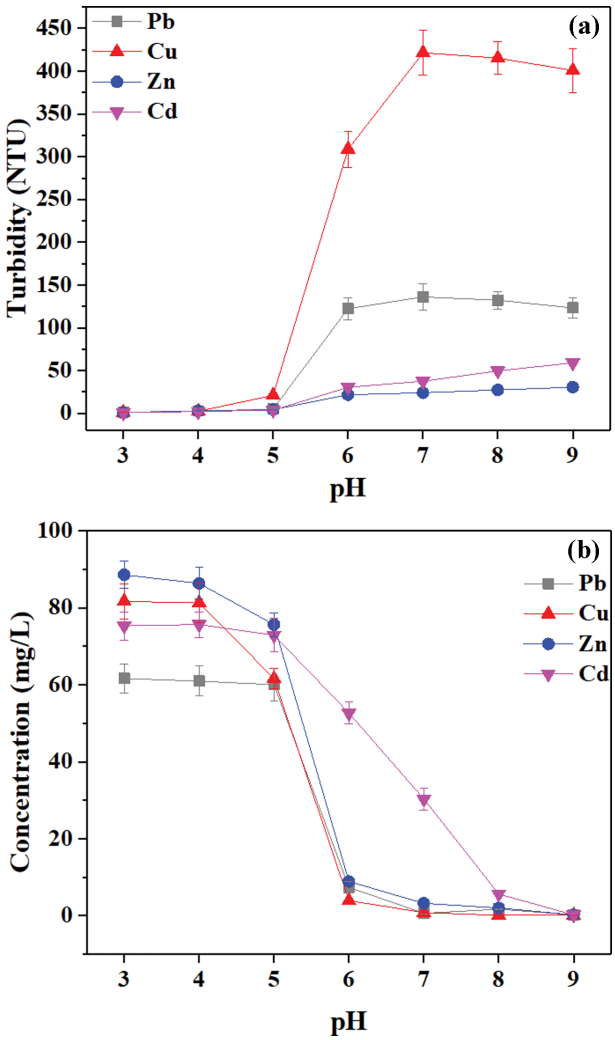


Fig. 10. Turbidity (a) and heavy metal concentration (b) of the suspensions after adsorption under different pH values.

Fig. 10 shows that the turbidity of the suspensions increased with the rise of the pH, mainly due to the precipitate formed when pH>5. Meanwhile, the concentration of heavy metals in the suspensions decreased as the pH rose. The turbidity of the suspensions decreased in the following sequence: Cu>Pb>Cd>Zn, which suggests that Cu and Pb precipitates were more likely to cause clogging in HPC substrates used in constructed wetlands or permeable pavement systems.

Therefore, most of the adsorbed heavy metals on the surface of the HPC and the precipitation formed were stable under neutral and alkaline conditions. Meanwhile, the precipitation formed might cause clogging problems in practical applications. When pH<6, the precipitate might be dissolved and lead to potential migration of the heavy metals.

CONCLUSIONS

Granular HPC was prepared and showed a large potential for the removal of Pb, Cu, Zn, and Cd ions in aqueous solutions. Both adsorption and precipitation were observed in the batch experi-

ments. Compared with precipitation, adsorption played a more important role in the initial stage of the removal process or at lower concentration. The HPC particles continued about three-day removal after two days of adsorption equilibrium. Besides the removal by precipitation, the maximum Langmuir adsorption capacity of HPC reached 132.27, 87.14, 123.43 and 112.05 mg/g for Pb, Cu, Zn, and Cd, respectively. When various heavy metals coexisted, the removal capacity followed the order of Cu>Pb>Cd>Zn.

In addition to precipitation in liquid phase, the main adsorption mechanism was mainly dominated by Ca^{2+} exchange and surface precipitation, which was suggested by XRD, SEM-EDS and released Ca^{2+} results.

In batch experiments, most of the removed heavy metals were stable under neutral and alkaline conditions. When cement-related materials containing HPC are employed for heavy metal removal in wastewater treatment applications, the precipitate might be dissolved under acidic conditions and lead to potential migration of the heavy metals.

ACKNOWLEDGEMENTS

This research was supported by the Key Research and Development Program of Shaanxi Province (Grant No. 2018ZDCXL-SF-31-6) and the Special Scientific Research Program of Shaanxi Provincial Education Department (Grant No. 21JK0716).

DATA AVAILABILITY STATEMENT

All relevant data are included in the paper or its Supporting Information.

SUPPORTING INFORMATION

Additional information as noted in the text. This information is available via the Internet at http://www.springer.com/chemistry/journal/11814.

REFERENCES

1. C. F. Carolin, P. S. Kumar, A. Saravanan, G. J. Joshiba and M. Naushad, *J. Environ. Chem. Eng.*, **5**, 2782 (2017).
2. S. Mnasri-Ghnimi and N. Frini-Srasra, *Appl. Clay Sci.*, **179**, 105151 (2019).
3. S. Wadhawan, A. Jain, J. Nayyar and S. K. Mehta, *J. Water Process Eng.*, **33**, 101038 (2020).
4. F. Fu and Q. Wang, *J. Environ. Manage.*, **92**, 407 (2011).
5. S. Bolisetty, M. Peydayesh and R. Mezzenga, *Chem. Soc. Rev.*, **48**, 463 (2019).
6. L. Huang, M. He, B. Chen and B. Hu, *J. Mater. Chem. A*, **4**, 5159 (2016).
7. J. E. Efome, D. Rana, T. Matsuura and C. Q. Lan, *Sci. Total Environ.*, **674**, 355 (2019).
8. R. Mukherjee, P. Bhunia and S. De, *Chem. Eng. J.*, **292**, 284 (2016).
9. Q. Chang, M. Zhang and J. Wang, *J. Hazard. Mater.*, **169**, 621 (2009).
10. Y. Gomravi, A. Karimi and H. Azimi, *Korean J. Chem. Eng.*, **38**, 1843 (2021).
11. M. K. Uddin, *Chem. Eng. J.*, **308**, 438 (2017).
12. H. Yanagisawa, Y. Matsumoto and M. Machida, *Appl. Surf. Sci.*, **256**, 1619 (2010).
13. P. Z. Ray and H. J. Shipley, *RSC Adv.*, **5**, 29885 (2015).
14. S. S. Fiyadh, M. A. AlSaadi, W. Z. Jaafar, M. K. AlOmar, S. S. Fayaed, N. S. Mohd, L. S. Hin and A. El-Shafie, *J. Clean. Prod.*, **230**, 783 (2019).
15. E. Da'na, *Micropor. Mesopor. Mater.*, **247**, 145 (2017).
16. N. Shao, S. Tang, Z. Liu, L. Li, F. Yan, F. Liu, S. Li and Z. Zhang, *ACS Sustain. Chem. Eng.*, **6**, 14926 (2018).
17. A. Mancini, E. Wieland, G. Geng, R. Dähn, J. Skibsted, B. Wehrli and B. Lothenbach, *Appl. Geochem.*, **113**, 104460 (2020).
18. B. Guo, K. Sasaki and T. Hirajima, *Cem. Concr. Res.*, **100**, 166 (2017).
19. D. Martemianov, B. B. Xie, T. Yurmazova, M. Khaskelberg, F. Wang, C. H. Wei and S. Preis, *J. Environ. Chem. Eng.*, **5**, 3930 (2017).
20. Y. S. Ok, J. E. Yang, Y. S. Zhang, S. J. Kim and D. Y. Chung, *J. Hazard. Mater.*, **147**, 91 (2007).
21. G. M. P. Kumara, K. Kawamoto, T. Saito, S. Hamamoto and S. Asamoto, *J. Environ. Eng.*, **145**, 04019078 (2019).
22. A. N. Shabalala, S. O. Ekolu, S. Diop and F. Solomon, *J. Hazard. Mater.*, **323**, 641 (2017).
23. R. R. Holmes, M. L. Hart and J. T. Kevern, *J. Contam. Hydrol.*, **196**, 52 (2017).
24. Z. T. Abd Ali, L. A. Naji, S. A. A. A. N. Almuktar, A. A. H. Faisal, S. N. Abed, M. Scholz, M. Naushad and T. Ahamad, *J. Water Process Eng.*, **33**, 101033 (2020).
25. M. El Zayat, S. Elagroudy and S. El Haggar, *Water Sci. Technol.*, **70**, 1011 (2014).
26. A. E. E. A. Z. Amin and S. A. H. Selmy, *Commun. Soil Sci. Plant Anal.*, **48**, 1301 (2017).
27. J. Staunton, C. D. Williams, L. Morrison, T. Henry, G. T. A. Fleming and M. J. Gormally, *Land Use Policy*, **49**, 43 (2015).
28. M. A. Rahman, M. A. Imteaz, A. Arulrajah, J. Piratheepan and M. M. Disfani, *J. Clean. Prod.*, **90**, 183 (2015).
29. M. A. Rahman, M. A. Imteaz, A. Arulrajah, M. M. Disfani and S. Horpibulsuk, *J. Environ. Eng.*, **141**, 04015019 (2015).
30. L. W. Gill, P. Ring, N. M. P. Higgins and P. M. Johnston, *Ecol. Eng.*, **70**, 133 (2014).
31. L. W. Gill, P. Ring, B. Casey, N. M. P. Higgins and P. M. Johnston, *Sci. Total Environ.*, **601**, 32 (2017).
32. M. Mondal and A. K. Ray, *Adsorption*, **26**, 387 (2020).
33. W. Guan, F. Ji, Q. Chen, P. Yan and Q. Zhang, *Ceram. Int.*, **39**, 1385 (2013).
34. M. Monier, D. M. Ayad, Y. Wei and A. A. Sarhan, *J. Hazard. Mater.*, **177**, 962 (2010).
35. S. Sen Gupta and K. G. Bhattacharyya, *J. Environ. Manage.*, **87**, 46 (2008).
36. H. Zhang, Z. Tong, T. Wei and Y. Tang, *Desalination*, **276**, 103 (2011).
37. T. C. Nguyen, P. Loganathan, T. V. Nguyen, S. Vigneswaran, J. Kandasamy and R. Naidu, *Chem. Eng. J.*, **270**, 393 (2015).
38. M. Niu, G. Li, L. Cao, X. Wang and W. Wang, *J. Clean. Prod.*, **256**, 120700 (2020).
39. D. Mitrogiannis, M. Psychoyou, I. Baziotis, V. J. Inglezakis, N. Koukouzas, N. Tsoukalas, D. Palles, E. Kamitsos, G. Oikonomou and G. Markou, *Chem. Eng. J.*, **320**, 510 (2017).
40. N. B. Singh, G. Nagpal, S. Agrawal and Rachna, *Environ. Technol.*

Innov., **11**, 187 (2018).
41. J. Zhao, J. Liu, N. Li, W. Wang, J. Nan, Z. Zhao and F. Cui, *Chem. Eng. J.*, **304**, 737 (2016).
42. H. Cho, D. Oh and K. Kim, *J. Hazard. Mater.*, **127**, 187 (2005).
43. Q. Chen, Y. Yao, X. Li, J. Lu, J. Zhou and Z. Huang, *J. Water Process Eng.*, **26**, 289 (2018).
44. P. Srivastava, B. Singh and M. Angove, *J. Colloid Interface Sci.*, **290**, 28 (2005).
45. C. Liu, R. Bai and Q. San Ly, *Water Res.*, **42**, 1511 (2008).
46. X. Chen, Y. Guo, S. Ding, H. Zhang, F. Xia, J. Wang and M. Zhou, *J. Clean. Prod.*, **207**, 789 (2019).
47. Y. Wang, Z.-w. Li, B. Huang, W.-g. Jiang, L. Guo, J.-q. Huang and G.-m. Zeng, *J. Cent. South Univ.*, **22**, 1269 (2015).
48. J. Zhang, H. Zhao, H. Cao, H. Li and Z. Li, *J. Environ. Sci. (China)*, **25**, 1719 (2013).
49. M. A. Trezza, *Mater. Res.*, **10**, 331 (2007).
50. G. S. dos Reis, P. S. Thue, B. G. Cazacliu, E. C. Lima, C. H. Sampaio, M. Quattrone, E. Ovsyannikova, A. Kruse and G. L. Dotto, *J. Clean. Prod.*, **256**, 120416 (2020).
51. P. Mandaliev, R. Dähn, J. Tits, B. Wehrli and E. Wieland, *J. Colloid Interface Sci.*, **342**, 1 (2010).

Supporting Information

Heavy metal removal from aqueous solution by granular hydrated Portland cement

Peng Cheng[*,,***], Yongxiang Ren[*,**,†], Lei Yang[*,**], Rituan Li[*,**], Xue Wang[*,**], Bin Li[****], and Honglin Yuan[*,**]**

*Key Laboratory of Northwest Water Resource, Environment and Ecology, MOE, Xi'an University of Architecture and Technology, Xi'an 710055, P. R. China
**Shaanxi Key Laboratory of Environmental Engineering, Xi'an University of Architecture and Technology, Xi'an 710055, P. R. China
***School of Civil Engineering, Nanyang Institute of Technology, Nanyang 473004, Henan Province, P. R. China
****Xi'an Botanical Garden, Xi'an 710061, Shaanxi Province, P. R. China
(*Received 28 February 2022 • Revised 27 June 2022 • Accepted 29 June 2022*)

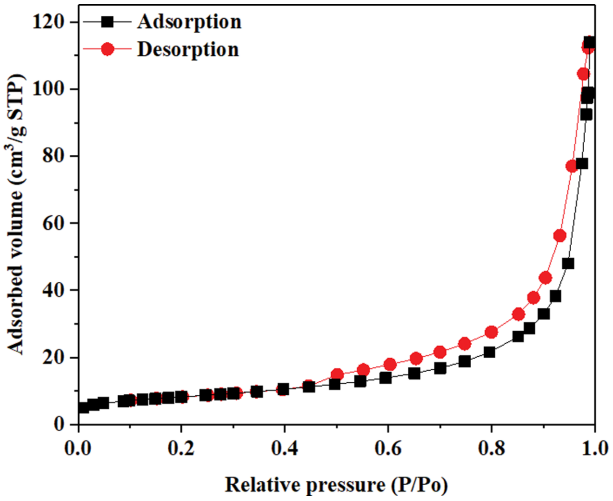


Fig. S1. N_2 adsorption–desorption isotherms of the prepared HPC.

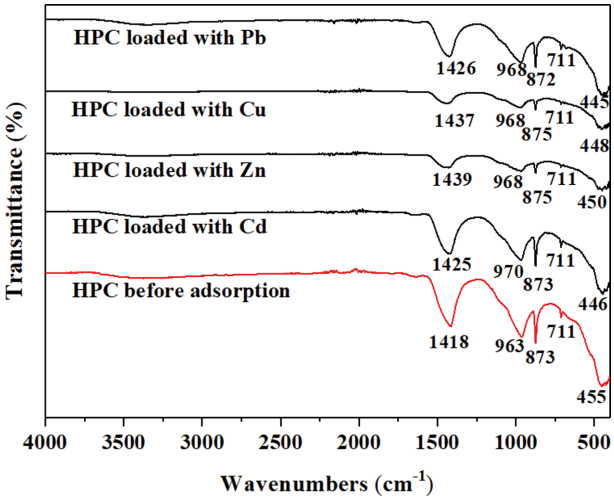


Fig. S2. FT-IR spectra of the HPC before and after heavy metals adsorption.

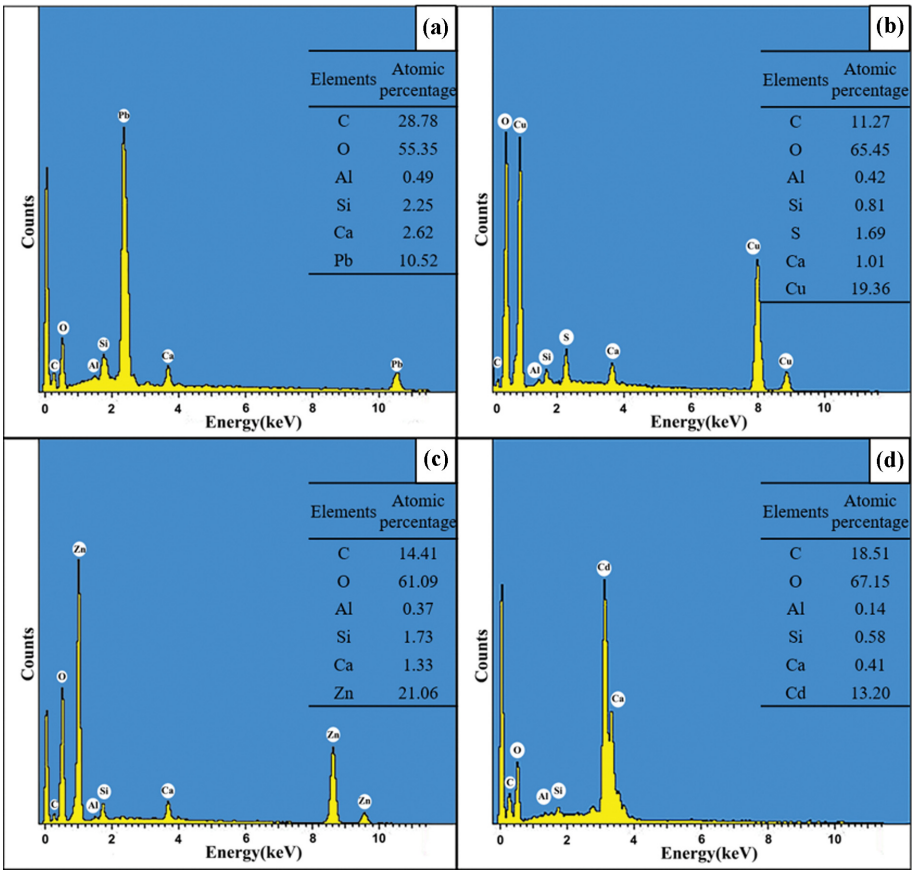


Fig. S3. EDS spectrum of HPC loaded with Pb (a), Cu (b), Zn (c), Cd (d).

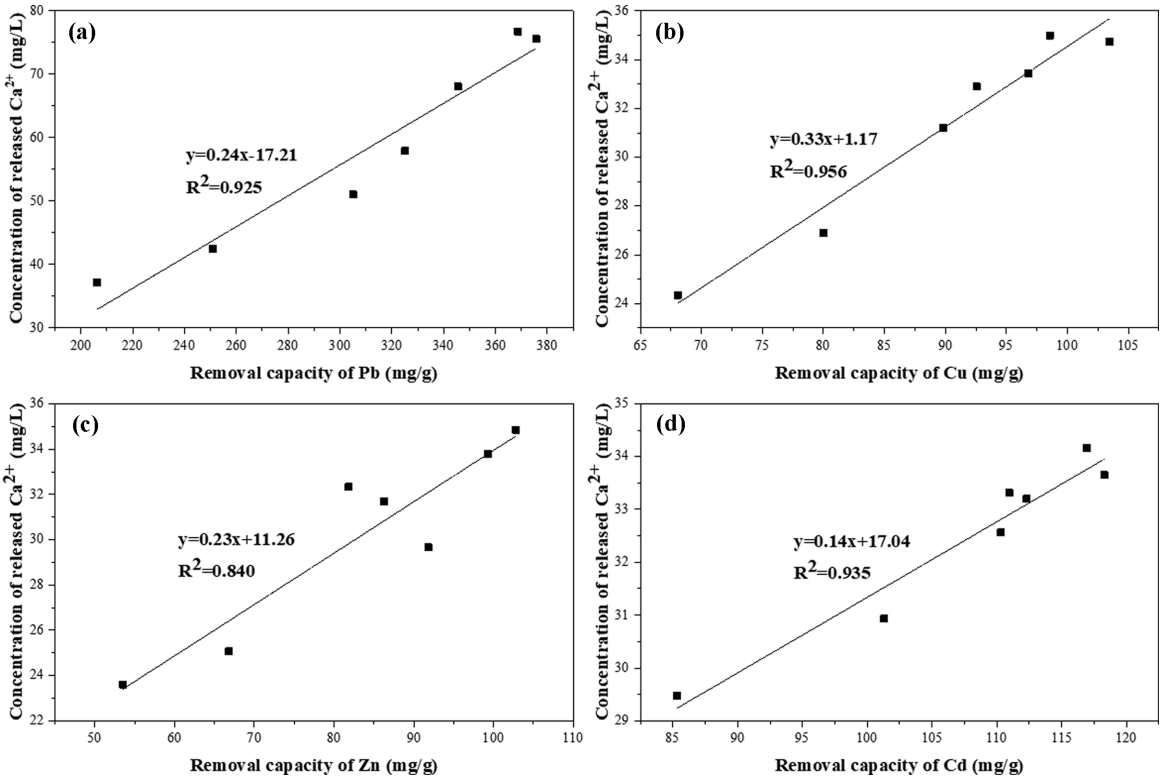


Fig. S4. Relationships between released Ca^{2+} concentration and the total removal capacities of Pb (a), Cu (b), Zn (c) and Cd (d).